NMRlipids IV: Headgroup & glycerol backbone structures, and cation binding in bilayers with PE and PG lipids

Pavel Buslaev,[1] Fernando Favela-Rosales,[2] Patrick Fuchs,[3] Matti Javanainen,[4] Jesper J. Madsen,[5,6] Josef Melcr,[4,7] Markus S. Miettinen,[8] O. H. Samuli Ollila,[9,*] Chris G. Papadopoulos,[10] Antonio Peón,[11] Thomas J. Piggot,[12] and Pierre Poulain[3]

[1]*University of Jyväskylä*
[2]*Departamento de Investigación, Tecnológico Nacional de México, Campus Zacatecas Occidente, México*
[3]*Paris, France*
[4]*Institute of Organic Chemistry and Biochemistry of the Czech Academy of Sciences, Flemingovo nám. 542/2, CZ-16610 Prague 6, Czech Republic*
[5]*Department of Chemistry, The University of Chicago, Chicago, Illinois, United States of America*
[6]*Department of Global Health, College of Public Health, University of South Florida, Tampa, Florida, United States of America*
[7]*Groningen Biomolecular Sciences and Biotechnology Institute and The Zernike Institute for Advanced Materials, University of Groningen, 9747 AG Groningen, The Netherlands*
[8]*Department of Theory and Bio-Systems, Max Planck Institute of Colloids and Interfaces, 14424 Potsdam, Germany*
[9]*Institute of Biotechnology, University of Helsinki*
[10]*I2BC - University Paris Sud*
[11]*Spain*
[12]*Chemistry, University of Southampton, Highfield, Southampton SO17 1BJ, United Kingdom*

(Dated: December 10, 2020)

The force field giving the best description for glycerol backbone and headgroup structures of PC, PS, PG and PE headgroups (CHARMM36) reproduces the essential differences in order parameters between these headgroups, and therefore enables the analysis of structural differences between the headgroups.

INTRODUCTION

Chemical compositions of hydrophilic lipid headgroups vary between different organelles and organisms, and different lipid types regulate protein functions in many different ways [1, 2]. Lipids can directly bind to proteins or indirectly affect protein functions by altering membrane properties or charge [1, 3]. While the specific interactions with certain lipid headgroups are known to be essential for the function of several proteins [3, 4], it is not clear if the specificity is driven by the differences in accessible conformational states between lipid types or by specific intermolecular lipid-protein interactions.

Lipid conformational ensembles in physiologically relevant lamellar liquid phase are typically derived from NMR experiments, particularly from C-H bond order parameters measured using ^{2}H NMR [5–7] which can be detected even from cells [8–10]. These studies suggest that the glycerol backbone structures are largely similar irrespectively of the headgroup [8], and the headgroup structures are similar in PC, PE and PG lipids, while headgroup is more rigid in PS lipids [11, 12]. However, these results are based only on the absolute values while the necessity of order parameters signs in capturing the lipid conformational ensembles has been resently demonstrated [13–15]. Furthermore, the detailed understanding of lipid conformational ensembles is limited by the lack of universal models to interpret the experiments [16, 17].

Stuctures of different lipid types in protein bound states can be extracted from the protein data bank (PDB) [18], but their relation to the conformational ensembles in liquid lamellar state remains unclear [19]. In addition to the changes in lipid conformational ensembles upon binding to proteins, also the experimentally measured response of lipid headgroup to membrane bound charges remains poorly understood due to the lack of suitable models to interpret the lipid conformational ensembles in liquid lamellar state [7].

Here, we use natural abundance ^{13}C NMR experiments and MD simulations from the NMRlipids open collaboration to resolve the differences in conformational ensembles between PC, PE, PG and PS lipid headgroups. Zwitterionic PC and PE are the most common lipids in eukaryotes and bacteria, respectively [2, 20]. PE is also the second most abundant glycerophospholipid in eukaryotic cells and has been related to various diseases [21–23]. PS and PG are the most common negatively charged lipids in eukaryotes and bacteria, respectively, and affect membrane protein functionality and signaling [3, 20, 24, 25]. All the studied lipids specifically bind to various proteins [26]. Furthermore, we use our results to elucidate lipid-protein interactions and the effect of charges on lipid conformations.

The lipid conformational ensembles in liquid lamellar state paves the way toward understanding the specific binding of different lipid types to membrane proteins and how they regulate the protein function. Because glycerol backbone and headgroup structures of PC lipids are similar in model membranes and in bacteria [8–10], the results from model systems could be used to understand the biological role of lipid headgroup conformational ensembles in different lipid types.

METHODS

Experimental C–H bond order parameters

The headgroup and glycerol backbone C–H bond order parameters of POPE and POPG were measured using natural abundance ^{13}C solid state NMR spectroscopy as described previously [15, 27]. The magnitudes of order parameters were determined from the chemical-shift resolved dipolar splittings using a R-type Proton Detected Local Field (R-PDLF) experiment [28] and the signs from S-DROSS experiments [29] combined with SIMPSON simulations [30]. The NMR experiments were identical as in our previous work [31]. POPE and POPG powder were purchased from Avanti polar lipids **1.Which isomer of POPG we have in the experiments?**. The POPE experiments were recorded at 310 K and POPG experiments at 298 K, where the bilayers are in the liquid disordered phase [32].

Glycerol backbone peaks from both lipids, and α-carbon peak from POPE in the INEPT spectra were assigned based on previously measured POPC spectra [27]. The β-carbon peak from POPE was assigned based on ^{13}C chemical shift table for amines available at `https://www.chem.wisc.edu/areas/reich/nmr/c13-data/cdata.htm`. **2.How were α and γ-carbon peaks assigned in POPG?**. The β-carbon peak from POPG overlapped with the g_2 peak from glycerol backbone because their chemical environments are similar in POPG. **3.Details to be checked by Tiago.**

Molecular dynamics simulations

Molecular dynamics simulation data were collected using the NMRlipids Open Collaboration [13], which is running at `nmrlipids.blogspot.fi` and `github.com/NMRlipids/NMRlipidsIVotherHGs`. The simulated systems of pure PE and PG bilayers without additional ions are listed in Tables S1 and S2, and lipid mixtures with additional ions in Table S4. Further simulation details are given in the SI, and the simulation data are indexed in a searchable database available at `www.nmrlipids.fi`, and in the NMRlipids/MATCH repository (`github.com/NMRlipids/MATCH`).

Analysis of molecular dynamics simulation data

The big data set of MD simulations was analysed in the NMRlipids databank manner. Unique naming convention for lipid atoms in each force field was defined using the mapping files and analysis for all simulations indexed in NMRlipids databank manner were performed using python codes.

The C–H bond order parameters were calculated directly from the carbon and hydrogen positions using the definition

$$S_{\mathrm{CH}} = \frac{1}{2}\langle 3\cos^2\theta - 1\rangle, \qquad (1)$$

where θ is the angle between the C–H bond and the membrane normal (taken to align with z, with bilayer periodicity in the xy-plane). Angular brackets denote average over all sampled configurations. The order parameters were first calculated averaging over time separately for each lipid in the system. The average and the standard error of the mean were then calculated over different lipids. Python programs that use the MDAnalysis library [33, 34] used for all atom simulations is available in Ref. 35 (`scripts/calcOrderParameters.py`). For united atom simulations, the trajectories with hydrogens having ideal geometry were constructed first using either buildH program [36] or (`scratch/opAAUA_prod.py`) in Ref. 35, and the order parameters were then calculated from these trajectories. This approach has been tested against trajectories with explicit hydrogens and the deviations in order parameters are small [36, 37].

4.BuildH program is now cited with a direct link to the GitHub repo. I think that a release to Zenodo would be nice in the final publication.

5.Maybe we should also shortly discuss here about the reasons for slight dependence of order parameter values on the method used to reconstruct hydrogens?

The ion number density profiles were calculated using the `gmx density` tool of the Gromacs sofware package [38].

Analysis of lipid conformations bound to proteins

Dihedral angles of all available conformations in the PDB databank were calculated using the API access to the databank.

RESULTS AND DISCUSSION

Conformational ensembles of different lipid headgroups in bulk bilayer

To experimentally characterize the headgroup conformational ensembles of lipids that are not bound to proteins in electrostatically neutral cell membrane, we measured the C-H bond order parameters and their signs from of POPG and POPE in liquid lamellar phase, as we did previously for POPC and POPS [15, 27, 31]. Determination of headgroup and glycerol backbone order parameters and their signs was straightforward from the data in Figs. 1, S1 and S2 for all the C-H bonds, except the β and g_2 carbons in POPG. These carbons have overlapping peaks in the INEPT spectra due to their similar chemical environments, and only the magnitude of the larger order parameter could be determined from the R-PDLF spectra (Fig. 1 B). Nevertheless, based on previous ^{2}H NMR measurements [8, 11, 40], we assigned the larger order parameter to the g_2 carbon and used the literature value for the β-carbon in SIMPSON simulations to determine the signs. The decrease in the beginning of the S-DROSS curve suggests that the sign of larger g_2 order parameter is negative and later increase suggests that sign of smaller β order parameter is pos-

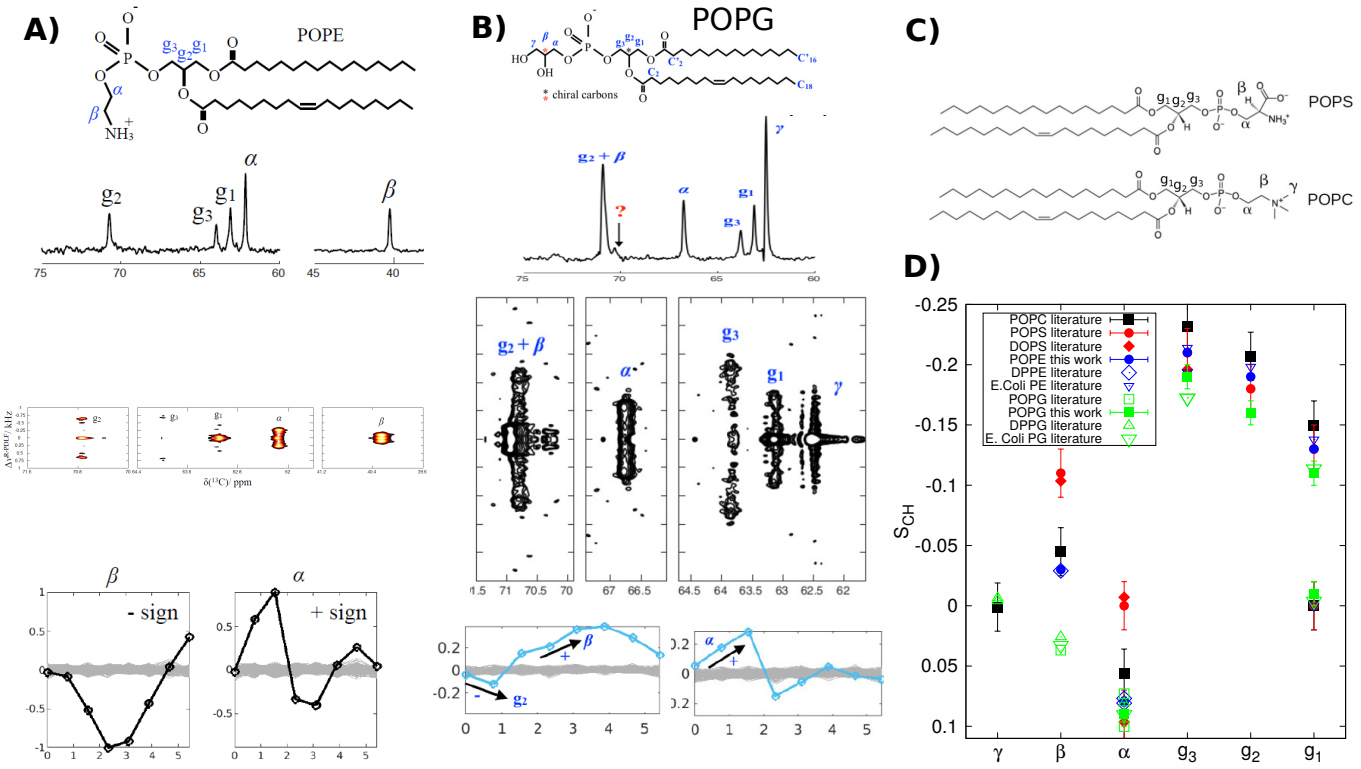

FIG. 1: Chemical structure, refocused-INEPT spectrum, 2D R-PDLF spectra, and S-DROSS data (from top to bottom) of **A)** POPE and **B)** POPG. Full NMR spectra are shown Figs. S1 and S2. **C)** Chemical structure of POPC and POPS. **D)** Headgroup and glycerol backbone order parameters from different experiments in lamellar liquid disordered phase. The values and signs for POPE (310 K) and POPG (298 K) measured in this work, and for POPS (298 K) [31] and POPC (300 K) [15, 27] previously using ^{13}C NMR. The literature values for DOPS with 0.1M of NaCl (303 K) [39], POPG with 10nM PIPES (298 K) [40], DPPG with 10mM PIPES and 100mM NaCl (314 K) [11], DPPE (341 K) [41], E.coliPE and E.coliPG (310 K) [8] are measured using ^{2}H NMR. The signs from ^{13}C NMR are used also for the literature values.

6.This is a sketch, Tiago Ferreira will make a new figure.

7.D) could be clarified as Fig. 2 in the NMRlipids IVps paper.

itive (Fig. 1 (B)). This interpretation is confirmed by SIMPSON calculations in Fig S3.

Experimental order parameters of POPC, POPE, POPG and POPS glycerol backbones and headgroups from this and previous studies are collected in Fig. 1 D), where signs determined from ^{13}C NMR experiments are used also for the ^{2}H NMR data from the literature. Overall agreement of order parameters determined by different authors and different techniques for same lipid headgroup is very good in here and previous studies [13, 14, 31], suggesting that the observed differences between lipid types arise from differences in headgroup chemistry rather than inaccuracies in experiments. The most distinct order parameters are observed for PS headgroups, for which the α-carbon order parameter exhibits significant forking and the β-carbon has more negative value than in other lipids. On the other hand, the β-carbon order parameter of PG headgroup has positive sign in contrast to all the other lipids. Notably, this has not been observed in traditional ^{2}H NMR experiments, where only the absolute value of the order parameters are measured [8, 11, 40]. The glycerol backbone order parameters are similar for all the lipids, although they move slightly toward positive values (closer to zero) in the order PC $<$ PE $<$ PS $<$ PG. Essential differences between PC and PE headgroups are not observed.

To resolve the conformational ensembles of lipid headgroups, we compared the headgroup and glycerol backbone C-H bond order parameters from different MD simulation force fields to the experimental data. None of the force fields reproduced the order parameters within experimental accuracy for any of the lipids analysed in this work (Figs. S4 and S5) or in our previous studies [13, 31]. Nevertheless, the CHARMM36 force field performs best for all the headgroups and reproduces the distinct order parameters of PS and PG lipids (Fig. 2 B). To understand the structural origin of these distinct order parameters, we calculated the distributions of heavy atom dihedral angles from CHARMM36 simulations in figure 2 C). Major differences between headgroups are observed only for the last two dihedrals in the headgroup end, O_α-C_α-C_β-N/C_γ and P-O_α-C_α-C_β, which prefer *gauche*$^-$ conformations for PG and *gauche*$^+$ for PS. Rest of the dihedrals are similar between different lipids, with the exception of small differences for PS lipids. Therefore we suggest that the main differences between lipid headgroups leading to distinct order parameter occur in the choline part, while also changes

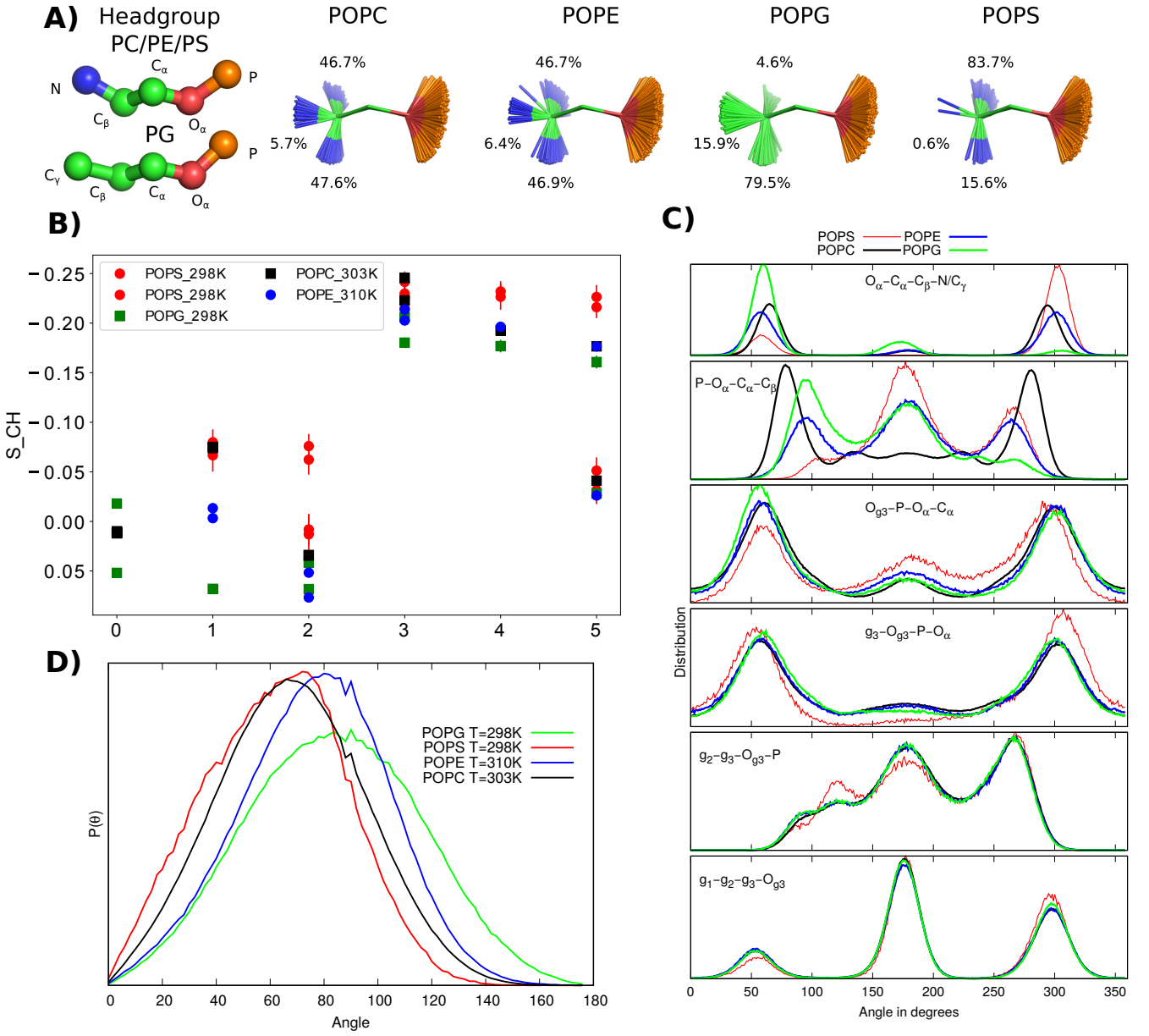

FIG. 2: Results from CHARMM36 simulations demonstrating the differences in conformational ensembles betwee different lipids. **A)** Snapshots with overlayed C_β, C_α and O_α atoms and occurence of different conformations. **B)** Headgroup and glycerol backbone region order parameters of different different lipids. **C)** Distributions of heavy atom dihedral angles of different lipids from CHARMM36 simulations. **D)** Distributions of P-N vector angle with respect to membrane normal.

8.This is a draft and requires quite a bit of polishing. More detailed discussion of this figure is in https://github.com/NMRLipids/NMRlipidsIVPEandPG/issues/9

in phosphate region may contribute in PS lipids, which could also explain the more rigid headgroup structures [12, 39]. Furthermore, the angle between headgroup dipole and membrane normal decreases in the order of PG > PE > PC > PS (Fig. 2 B)). However, the differences between PC and PE in P-O_α-C_α-C_β dihedral and P-N vector dipole may be an artefacts as the β-carbon order parameter in PC is too negative the CHARMM36 force field, thereby not being equal to the order parameter in PE as observed in experiments [13].

In conclusion, all lipid headgroups sample very broad conformational ensembles in liquid lamellar phase. Despite the differences in distributions between headgroups, the sampled dihedral angles are within approximately same ranges for all headgroup types. Therefore, we suggest that all lipid headgroups are very flexible thereby being able to adopt wide range of multiple conformations when interacting with proteins, ions or other biomolecules. Our results support the models that propose free rotation around phosphate group for PC lipids, which decouples the dynamics and conformatios between acyl chains and headgroups [42, 43], and suggests

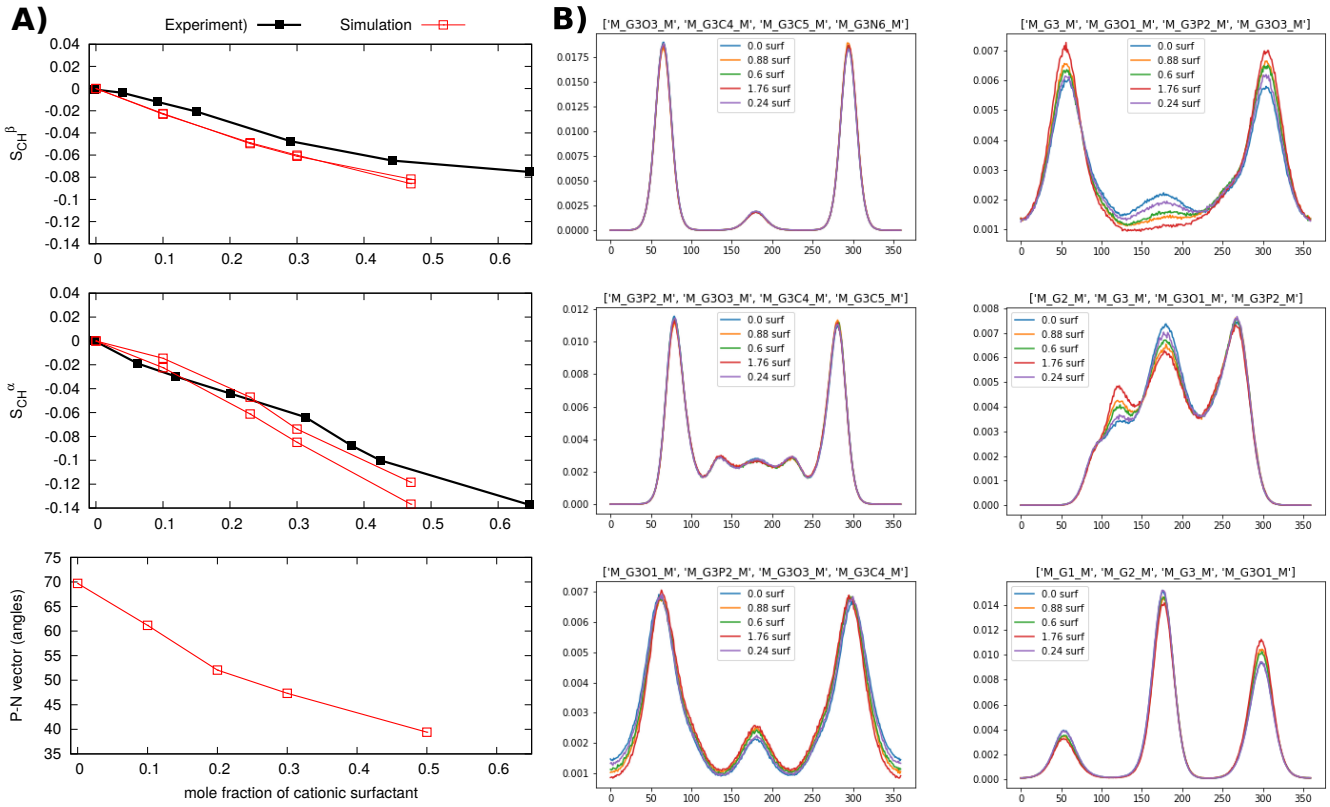

FIG. 3: **A)** Modulation of PC headgroup order parameters and P-N vector angle upon addition of cationic surfactant from CHARMM36 simulations compared with experimental data [**?**]. **B)** Changes in PC headgroup conformational ensembles upon increasing amount of positive charge in bilayer, characterized by the heavy atom dihedral distributions, from CHARMM36 simulations.

that these models could be applied for all lipids containing the phosphorus group. The wide range of observed conformations suggest that the structures in lipid crystals [12, 44] play only a minor role, and that the models aiming to explain NMR data using only few conformations [5–7, 17] are not sufficient to capture the large conformational space of lipids in liquid lamellar state.

Lipid conformational ensembles in lipid bilayers with bound ions

Charged lipids, proteins, surfactants, drugs, and ions incorporated in membranes reorient the headgroup dipole in PC lipids, thereby affecting the order parameters of lipid headgroups [45]. However, detailed understanding on lipid conformational ensembles in membranes bearing electric charge is still lacking [7].

To resolve lipid headgroup conformational ensembles in cell membrane bearing positive charge, we first analyzed CHARMM36 simulations which correctly capture the experimentally measured decrease in PC headgroup order parameters upon addition of cationic surfactants into a bilayer in figure 3 A). Heavy atom dihedral angle distributions in figure 3 B reveal that the decrease of trans state probabilities in g_2-g_3-O_{g_3}-P and g_3-O_{g_3}-P-O_α dihedrals are the major effects of positive charge on lipid headgroup conformations. Choline region remains essentially unchanged and only minor changes are observed in other dihedrals even thought almost half of the molecules in membranes are cationic surfactants. We also tried to resolve PC lipid headgroup conformational ensembles in mixed membrane with negatively charged lipids [9], but the accuracy of currently available force fields was not sufficient for this (Fig. S6).

Also binding of ions may affect the zwitterionic and charged lipid headgroup conformational ensembles in physiological conditions. The resolve this effect, we compared the changes of headgroup order parameters in POPC:POPG mixtures upon addition of $CaCl_2$ between different simulations and experiments [40, 46] in figures 4 (molar ratio 1:1) and S9 (molar ratio 4:1). As in our previous studies [31, 48**?** , 49], the calcium binding affinity to membranes is typically overestimated in simulations, except by CHARMM36 with the NBfix correction which underestimates the binding affinity, and the implicit inclusion of electronic polarizability improves the results. Lipid17ecc model with the implicit inclusion of electronic polarizability gives the most realistic response of PC lipid headgroup order parameters to the binding of calcium. In this model, the main effect of calcium to the lipid

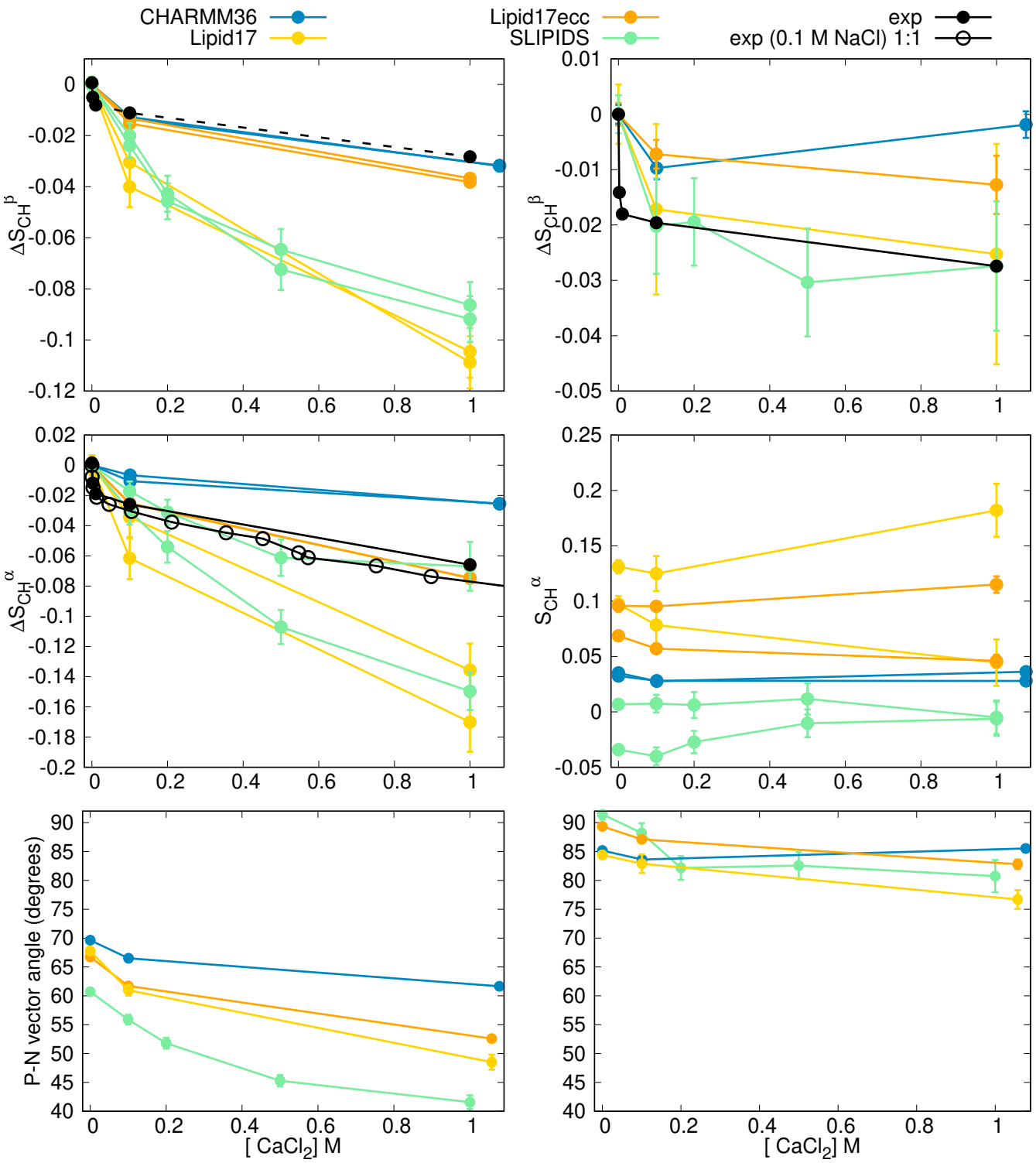

FIG. 4: Modulation of headgroup order parameters of POPC (*left*) and POPG (*right*) in POPC:POPG (1:1) mixture upon addition of $CaCl_2$ in 298 K temperature from experiments [40, 46] and simulations. The β-carbon order parameter of POPC (dashed line on top left) is not directly measured but calculated from empirical relation $\Delta S_\beta = 0.43\Delta S_\alpha$ [47]. The changes with respect to the systems without $CaCl_2$ are shown for other data than for the α-carbon of POPG for which experimental order parameter is not available. Calsium density distributions are shown in figure S8.

conformational ensemble is the slight change of g_3-O_{g3}-P-O_α dihedral distribution from trans state to eclipsed conformations (Fig. S12). This is in line with the changes observed in CHARMM36 simulations upon addition of charged surgactants (Fig. 3), despite the major differences in lipid headgroup conformational ensembles between these models without ions (Fig. 2 vs. Fig. S12).

Decrease in headgroup order parameters of PC lipids upon addition of charges is usually qualitatitely captured in simulations despite the inaccuries in lipid conformational ensembles [48], but situation with PS lipids is more complicated [31**?**]. Here, Lipid17 and Slipids force fields correctly capture the PG β-carbon order parameter response to $CaCl_2$ in figure 4 even thought the calcium binding affinity was overestimated. Heavy atom dihedral angle distributions calculated from these simulations suggest that also the headgroup glycerol conformations in PG are affected by calcium (Figs S13 and S14), in contrast to PC lipids where only conformations near phosphate were affected. On the other hand, the upward tilting of the headgroup dipole is weaker in PG than in PC headgroup, possible due to the compensating effects from the changes in phosphate and glycerol regions. However, none of the simulations captures and calcium binding affinity and conformational ensemble of PG lipids simultaneously, and experimental data to evaluate the response of α-carbon order parameters to the added calcium in PG is not available. Therefore, more accurate force fields are required for the solid analysis of PG conformations enembles in different ionic conditions.

Despite the limited cabability of simulations to interpret some experimental data due to the inaccuries in force fields, we can conclude that the experimentally observed changes in headgroup order parameters upon addition of charges into bilayer arise from relatively small changes in conformational ensembles. These changes can be characterised by mild changes in dihedral angle distributions, rather than restriction of lipids into fixed conformations. Therefore, lipid headgroups remain in disordered state sampling large space of different conformations, thereby being able to interact with different molecules in various ways, also when charged molecules are bound to membranes.

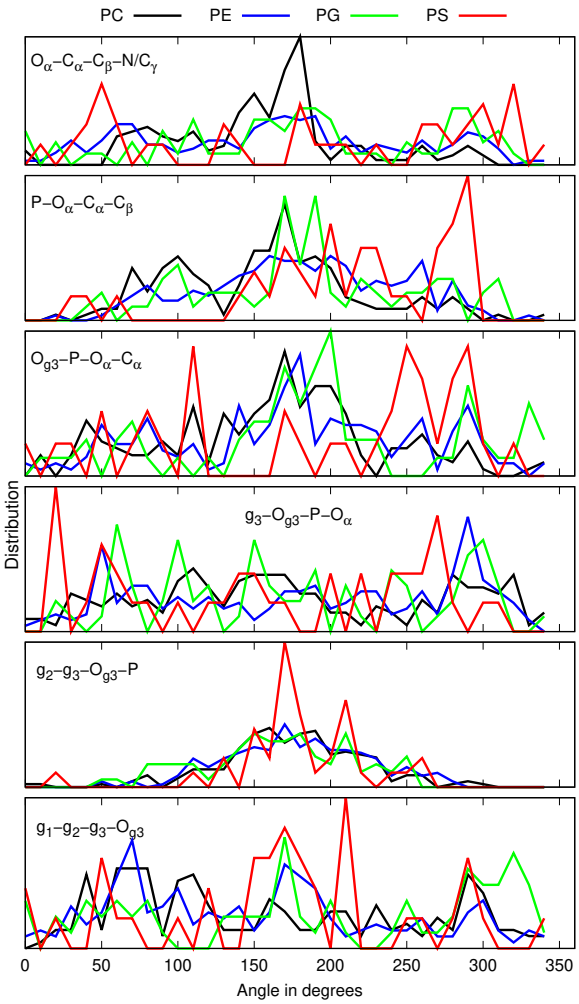

FIG. 5: Dihedral distributions from simulations and lipid structures in PDB.

Protein bound lipid conformations

While our results in previous sections suggest that lipid headgroups sample large conformational space in liquid lamellar phase, lipids can bound to proteins in fixed conformations which can be then detected using crystallography or cryo-EM. Such protein bound lipid conformations are available within protein structures deposited in The Protein Data Bank (PDB) available at `http://www.rcsb.org/` [18]. With our criterias described in the methods, we found ?? conformations of PC lipids, ?? conformations of PE lipids, ?? conformations of PG lipids, and ?? conformations of PS lipids from PDB.

To analyze the relation of lipid headgroup conformational ensembles between liquid lamellar and protein bound states, we calculated the heavy atom dihedral angle distributions also from the protein conformations found from the PDB. The results in figure 5 do not reveal major differences between different lipid headgroups when bound to proteins. Some preference for trans state in C_α-C_β bond of PC lipids, and for positive angles in O_α-C_α and P-O_α of PS lipids with respect to other lipids may be present in the data, but more statistics is required for solid conclusions. Therefore, the differences in conformational ensembles between different lipids observed in liquid lamellar state are not clearly visible in the protein bound states.

Almost all dihedral angles are found from the protein bounds states for all dihedrals except for P-O_α-C_α-C_β and g_2-g_3-O_{g_3}-P, which seem to avoid the cis conformations. The wide range of available dihedrals is similar to our results in liquid lamellar state, except for O_α-C_α-C_β-/C_γ and g_1-g_2-g_3-O_{g_3} dihedrals which seem to be more restricted in the liquid lamellar phase (Fig. 2). This suggests that lipids compromize their preferred conformations when bound to proteins to min-

imize the intermolecular interactions with proteins.

CONCLUSIONS

We have measured the C-H bond order parameters with the signs for headgroup and glycerol backbone regions of the most most abundant biological phopholipids, PC, PE, PG and PS. Combining this experimental data with the large amount of simulation data collected using the NMRlipids open collaboration, we were able to resolve the differences between conformational ensembles of lipid headgroup leading to the differences observed in NMR experiments.

Our results indicate that lipid headgroups are flexible and sample large conformational space in biologically relevant liquid lamellar state, also in membranes containing charged molecules, which have the largest affect on lipid headgroups in NMR experiments. Therefore, lipids can bind to proteins and other biomolecules in multiple different conformations, as indeed observed in the analysis of protein bound lipid conformations available from PDB. The weak correlation between lipid structures in liquid lamellar phase and protein bound state suggestst that the selective lipid binding to proteins is dominated by the intermolecular lipid-protein interactions, and the differences in conformational ensembles between different lipid types play only a minor role.

Our results pave the way to understand how lipids regulate membrane protein function. For example, the resolved lipid conformational ensembles in liquid lamellar phase and realistic MD simulations enables accurate analysis of lipid-protein interactions energetics. Furthermore, our results demonstrate how NMR data can be combined with the large amount of indexed MD simulation data to find the most realistic conformational ensembles of biomolecules in membrane environment. This paves the way toward standardized methods to resolve the quality evaluated conformational ensembles of disordered biomolecules in membrane environment. In the NMRlipids project we aim to build a general databank of quality evaluated conformational ensembles of lipids and other disordered biomolecules based primarily on MD simulations and NMR data.

AP is grateful to the Centro de Supercomputacin de Galicia (CESGA) for use of the Finis Terrae computer

* samuli.ollila@helsinki.fi

[1] A. Lee, Biochimica et Biophysica Acta (BBA) - Biomembranes **1612**, 1 (2003), ISSN 0005-2736, URL http://www.sciencedirect.com/science/article/pii/S0005273603000567.

[2] G. van Meer, D. R. Voelker, and G. W. Feigenson, Nature Reviews Molecular Cell Biology **9**, 112 (2008), URL https://doi.org/10.1038/nrm2330.

[3] M. A. Lemmon, Nat. Rev. Mol. Cell Biol. **9**, 99 (2008).

[4] A. G. Lee, Trends in Biochemical Sciences **36**, 493 (2011), URL https://doi.org/10.1016/j.tibs.2011.06.007.

[5] J. Seelig, Q. Rev. Biophys. **10**, 353 (1977).

[6] J. H. Davis, Biochim. Biophys. Acta **737**, 117 (1983).

[7] D. J. Semchyschyn and P. M. Macdonald, Magn. Res. Chem. **42**, 89 (2004).

[8] H. U. Gally, G. Pluschke, P. Overath, and J. Seelig, Biochemistry **20**, 1826 (1981).

[9] P. Scherer and J. Seelig, EMBO J. **6** (1987).

[10] J. Seelig, Cell Biology International Reports **14**, 353 (1990), ISSN 0309-1651, URL http://www.sciencedirect.com/science/article/pii/030916519091204H.

[11] R. Wohlgemuth, N. Waespe-Sarcevic, and J. Seelig, Biochemistry **19**, 3315 (1980).

[12] G. Büldt and R. Wohlgemuth, The Journal of Membrane Biology **58**, 81 (1981), ISSN 1432-1424, URL http://dx.doi.org/10.1007/BF01870972.

[13] A. Botan, F. Favela-Rosales, P. F. J. Fuchs, M. Javanainen, M. Kanduč, W. Kulig, A. Lamberg, C. Loison, A. Lyubartsev, M. S. Miettinen, et al., J. Phys. Chem. B **119**, 15075 (2015).

[14] O. S. Ollila and G. Pabst, Biochimica et Biophysica Acta (BBA) - Biomembranes **1858**, 2512 (2016).

[15] T. M. Ferreira, R. Sood, R. Bärenwald, G. Carlström, D. Topgaard, K. Saalwächter, P. K. J. Kinnunen, and O. H. S. Ollila, Langmuir **32**, 6524 (2016).

[16] W. Pezeshkian, H. Khandelia, and D. Marsh, Biophysical Journal **114**, 1895 (2018), ISSN 0006-3495, URL http://www.sciencedirect.com/science/article/pii/S0006349518302467.

[17] H. Akutsu, Biochimica et Biophysica Acta (BBA) - Biomembranes **1862**, 183352 (2020), URL https://doi.org/10.1016/j.bbamem.2020.183352.

[18] H. M. Berman, J. Westbrook, Z. Feng, G. Gilliland, T. N. Bhat, H. Weissig, I. N. Shindyalov, and P. E. Bourne, Nucleic Acids Research **28**, 235 (2000), ISSN 0305-1048, https://academic.oup.com/nar/article-pdf/28/1/235/9895144/280235.pdf, URL https://doi.org/10.1093/nar/28.1.235.

[19] D. Marsh and T. Páli, European Biophysics Journal **42**, 119 (2013), URL https://doi.org/10.1007/s00249-012-0816-6.

[20] C. Sohlenkamp and O. Geiger, FEMS Microbiology Reviews **40**, 133 (2015).

[21] J. E. Vance, Traffic **16**, 1 (2015).

[22] E. Calzada, O. Onguka, and S. M. Claypool (Academic Press, 2016), vol. 321 of *International Review of Cell and Molecular Biology*, pp. 29 – 88.

[23] D. Patel and S. N. Witt, Oxidative Medicine and Cellular Longevity **2017**, 4829180 (2017).

[24] P. A. Leventis and S. Grinstein, Annual Review of Biophysics **39**, 407 (2010).

[25] P. Hariharan, E. Tikhonova, J. Medeiros-Silva, A. Jeucken, M. V. Bogdanov, W. Dowhan, J. F. Brouwers, M. Weingarth, and L. Guan, BMC Biology **16**, 85 (2018).

[26] P. L. Yeagle, Biochimica et Biophysica Acta (BBA) - Biomembranes **1838**, 1548 (2014), membrane Structure and Function: Relevance in the Cell's Physiology, Pathology and Therapy.

[27] T. M. Ferreira, F. Coreta-Gomes, O. H. S. Ollila, M. J. Moreno, W. L. C. Vaz, and D. Topgaard, Phys. Chem. Chem. Phys. **15**, 1976 (2013).

[28] S. V. Dvinskikh, H. Zimmermann, A. Maliniak, and D. Sandstrom, J. Magn. Reson. **168**, 194 (2004).

[29] J. D. Gross, D. E. Warschawski, and R. G. Griffin, J. Am. Chem.

Soc. **119**, 796 (1997).
[30] M. Bak, J. T. Rasmussen, and N. C. Nielsen, Journal of Magnetic Resonance **147**, 296 (2000), ISSN 1090-7807, URL http://www.sciencedirect.com/science/article/pii/S1090780700921797.
[31] H. S. Antila, P. Buslaev, F. Favela-Rosales, T. Mendes Ferreira, I. Gushchin, M. Javanainen, B. Kav, J. J. Madsen, J. Melcr, M. S. Miettinen, et al., The Journal of Physical Chemistry B p. acs.jpcb.9b06091 (2019), ISSN 1520-6106.
[32] D. Marsh, *Handbook of Lipid Bilayers, Second Edition* (RSC press, 2013).
[33] N. Michaud-Agrawal, E. J. Denning, T. B. Woolf, and O. Beckstein, Journal of Computational Chemistry **32**, 2319 (2011), https://onlinelibrary.wiley.com/doi/pdf/10.1002/jcc.21787, URL https://onlinelibrary.wiley.com/doi/abs/10.1002/jcc.21787.
[34] Richard J. Gowers, Max Linke, Jonathan Barnoud, Tyler J. E. Reddy, Manuel N. Melo, Sean L. Seyler, Jan Domaski, David L. Dotson, Sbastien Buchoux, Ian M. Kenney, et al., in *Proceedings of the 15th Python in Science Conference*, edited by Sebastian Benthall and Scott Rostrup (2016), pp. 98 – 105.
[35] ohsOllila and et al., *Match github repository*, URL https://github.com/NMRLipids/MATCH.
[36] P. Fuchs and et al., *Buildh github repository*, URL https://github.com/patrickfuchs/buildH.
[37] T. J. Piggot, J. R. Allison, R. B. Sessions, and J. W. Essex, J. Chem. Theory Comput. **13**, 5683 (2017).
[38] M. Abraham, D. van der Spoel, E. Lindahl, B. Hess, and the GROMACS development team, *GROMACS user manual version 5.0.7* (2015), URL www.gromacs.org.
[39] J. L. Browning and J. Seelig, Biochemistry **19**, 1262 (1980).
[40] F. Borle and J. Seelig, Chemistry and Physics of Lipids **36**, 263 (1985).
[41] J. Seelig and H. U. Gally, Biochemistry **15**, 5199 (1976).
[42] J. B. Klauda, M. F. Roberts, A. G. Redfield, B. R. Brooks, and R. W. Pastor, Biophys. J. **94**, 3074 (2008).
[43] H. S. Antila, A. Wurl, O. H. S. Ollila, M. S. Miettinen, and T. M. Ferreira, *Quasi-uncoupled rotational diffusion of phospholipid headgroups from the main molecular frame* (2020), 2009.06774.
[44] I. Pascher, M. Lundmark, P.-G. Nyholm, and S. Sundell, Biochim. Biophys. Acta **1113**, 339 (1992).
[45] J. Seelig, P. M. MacDonald, and P. G. Scherer, Biochemistry **26**, 7535 (1987).
[46] P. M. Macdonald and J. Seelig, Biochemistry **26**, 1231 (1987).
[47] H. Akutsu and J. Seelig, Biochemistry **20**, 7366 (1981).
[48] A. Catte, M. Girych, M. Javanainen, C. Loison, J. Melcr, M. S. Miettinen, L. Monticelli, J. Maatta, V. S. Oganesyan, O. H. S. Ollila, et al., Phys. Chem. Chem. Phys. **18**, 32560 (2016).
[49] J. Melcr, H. Martinez-Seara, R. Nencini, J. Kolafa, P. Jungwirth, and O. H. S. Ollila, The Journal of Physical Chemistry B **122**, 4546 (2018).

ToDo